fire

Article

Data-Driven Prediction Methods for Real-Time Indoor Fire Scenario Inferences

Lu Zhang [1,2], Like Mo [1,2,3], Cheng Fan [1,2,3,*], Haijun Zhou [2] and Yangping Zhao [2]

[1] Sino-Australia Joint Research Center in BIM and Smart Construction, Shenzhen University, Shenzhen 518000, China; zl254619488@163.com (L.Z.); mlk@szu.edu.cn (L.M.)
[2] College of Civil and Transportation Engineering, Shenzhen University, Shenzhen 518000, China; haijun@szu.edu.cn (H.Z.); yangping@szu.edu.cn (Y.Z.)
[3] Key Laboratory for Resilient Infrastructures of Coastal Cities, Ministry of Education, Shenzhen University, Shenzhen 518000, China
* Correspondence: fancheng@szu.edu.cn

Abstract: High temperatures, toxic gases, and smoke resulting from indoor fires pose evident threats to the lives of both trapped individuals and firefighters. This study aims to predict indoor fire development effectively, facilitating rapid rescue decisions and minimizing casualties and property damage. A comprehensive database has been developed using Computational Fluid Dynamics (CFD) tools, primarily focused on basic fire scenarios. A total of 300 indoor fire scenarios have been simulated for different fire locations and severity levels. Using fire databases developed from simulation tools, artificial intelligence models have been developed to make spatial–temporal inferences on indoor temperature, CO concentration, and visibility. Detailed analysis has been conducted to optimize sensor system layouts while investigating the variations in prediction accuracy according to different prediction horizons. The research results show that, in combination with artificial intelligence models, the optimized sensor system can accurately predict temperature distribution, CO concentration, and visibility, achieving R^2 values of 91%, 72%, and 83%, respectively, while reducing initial hardware costs. The research results confirm the potential of artificial intelligence in predicting indoor fire scenarios and providing practical guidelines for smart firefighting. However, it is important to note that this study has certain limitations, including the scope of fire scenarios, data availability, and model generalization and interpretability.

Keywords: indoor fire; artificial intelligence; fire detection and deduction; CFD simulation; building safety

Citation: Zhang, L.; Mo, L.; Fan, C.; Zhou, H.; Zhao, Y. Data-Driven Prediction Methods for Real-Time Indoor Fire Scenario Inferences. *Fire* **2023**, *6*, 401. https://doi.org/10.3390/fire6100401

Academic Editors: Qiang Wang, Zihe Gao, Jinlong Zhao and Yongzheng Yao

Received: 3 August 2023
Revised: 6 October 2023
Accepted: 9 October 2023
Published: 18 October 2023

1. Introduction

Fire is a major disaster in the maintenance of buildings and infrastructure that can cause serious consequences, including loss of life, property, and facilities. With the majority of people spending their time indoors [1], indoor fire safety is crucial. In 2022, China experienced a notable surge in fire alarm cases and property loss, as reported by the National Fire and Rescue Administration, underscoring the urgent need for effective prediction and guidance in rescue and firefighting operations. The advancement of Industry 4.0 has enabled the integration of technologies like the Internet of Things (IoT), artificial intelligence (AI), big data analytics, and cloud computing in building systems, facilitating more intelligent operations [2–5]. These technological advancements have the potential to enhance fire prevention, detection, and response capabilities, reducing the adverse effects of fires. Timely and accurate prediction of fires is essential in guiding accurate fire rescue strategies, personnel evacuation plans, and intelligent fire rescue systems.

In the field of fire practice and scientific research, real-time monitoring of key features such as images, temperature, and smoke is commonly used for identifying and predicting indoor fires. Among these, image-based techniques for fire detection have been flourishing [6–8]. However, these methods often raise privacy concerns, and their performance can be severely compromised by camera malfunctions or poor image quality during fire events [9]. In addition, some studies have also used algorithms such as artificial neural networks for fire recognition based on environment-specific physical parameters like room temperature, thus avoiding the limitations of image quality. For instance, Wu et al. [10] succeeded in pinpointing tunnel fire location, fire severity levels, and ventilation wind speed with a precision of 90% by implementing Long Short-Term Memory (LSTM) models on temperature data.

Real-time prediction of the spatial and temporal development of indoor fires is crucial for supporting personnel evacuation and rescue operations, as well as enabling intelligent firefighting. So far, few studies have used sensor data to predict the key situation of indoor fires based on AI. Su et al. [11] developed an artificial intelligence model that can accurately predict smoke visibility profiles and available safety egress time for atrium fires. However, obtaining parameters such as fire size, smoke removal rate, and fire start time for prediction in real time remains challenging. Furthermore, Wu et al. [12] proposed a combined LSTM and Transpose Convolution Neural Network (TCNN) model for real-time prediction of the temperature distribution field in underground tunnels. By inputting sensor temperature data, the model outputs a predicted temperature field image with approximately 97% accuracy for temperature fields predicted 60 s ahead of time. While this research has made significant contributions in predicting temperature distributions, there remains a need for further advancements in predicting toxic gas concentrations and smoke visibility, which represent critical aspects of indoor fire scenarios. Moreover, it is important to address the limitations of existing research inference models. These models typically output grayscale or color images, which are subsequently inversely normalized to obtain corresponding temperature values based on pixel values. It is worth noting that grayscale images exhibit lower prediction quality, while color images offer higher-quality predictions but at the cost of longer model training times. Therefore, there is a clear demand for more reliable AI models capable of rapidly and swiftly predicting multiple fire-related parameters.

This paper focuses on the value of AI-enabled data-driven models in predicting critical indoor fire characteristics, including the spatial distribution of temperature, CO concentration, and smoke visibility, based on which optimal sensor layouts can be derived for practical applications. More specifically, a comprehensive numerical simulation database is firstly developed to simulate indoor fire scenarios with various fire locations and severity levels. Deep learning models are then trained to accurately predict the temperature distribution, CO concentration distribution, and smoke visibility distribution. The resulting model accuracies are used to evaluate the performance of different sensor layouts, aiming to ensure the cost-effectiveness of fire monitoring systems. Additionally, the study investigates the influence of different prediction horizons on the effectiveness of predictions. In discussing our findings, we also thoroughly discuss the limitations of this study, which include factors such as the scope of the fire scenarios, data availability, and model generalization and interpretability.

2. Research Methodology

2.1. Research Outline

Figure 1 shows the research outline. First, numerical simulations based on CFD tools are conducted to generate fire scenario databases with different fire locations and severity levels. Secondly, data preprocessing is performed to transform the original simulation data into suitable formats for predictive modeling. Thirdly, data experiments are designed to investigate the prediction performance of AI models considering different sensor data availabilities and prediction horizons. Comparative studies are then performed to derive suggestions on cost-effective solutions for smart fire prediction.

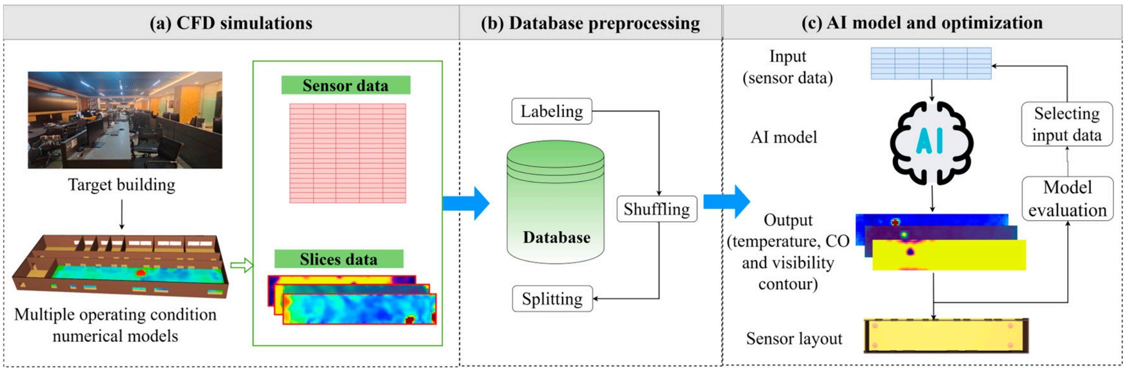

Figure 1. Research framework: (**a**) CFD simulations, (**b**) Database preprocessing, (**c**) AI model and optimization.

2.2. Basics on Numerical Simulation Models

Given the difficulty of conducting real fire experiments in situ, numerical simulation techniques are employed in this study to construct physical models and execute computations that facilitate AI-based fire predictions using the simulation data [13,14]. The Computational Fluid Dynamics (CFD) models are established using PyroSim, a Fire Dynamics Simulation (FDS) software developed by the National Institute of Standards and Technology (NIST) [15]. The outstanding feature of PyroSim is its provision of a 3D graphical pre-processing function, freeing users from the tedious and complex command line, enabling the rapid and precise setup of intricate fire models, and invoking FDS for simulation calculation. As a professional fire dynamics software, this tool can calculate and output numerous fire-related results, compute the relevant data of all grids at each time step, and offer abundant post-processing functions to preserve the calculated results. Previous studies have demonstrated the validity and reliability of CFD fire simulation data, making PyroSim a favored tool for fire simulation research [16–18]. In our previous study, we conducted numerical simulations and corresponding fire experiments in an experimental utility tunnel located in Yichang, Hubei. These experiments were conducted under different fire conditions. The validation results showed an agreement coefficient of about 75% between the two datasets. Considering these factors, such as wind speed instability and manual reading errors during the experiments, we can consider the fire data obtained from CFD numerical simulations to be accurate and valid.

2.3. Basics on Deep Learning Algorithms

The study utilizes deep learning algorithms such as LSTM, Convolutional Neural Network (CNN), and TCNN for analysis. This section briefly describes the algorithmic foundation of the model.

2.3.1. Long Short-Term Memory

Recurrent Neural Networks (RNNs) are a type of neural network that excels at processing sequential data. LSTM is a special type of RNN which can better capture long-term correlations in time-series data and overcomes challenges such as the diminishing and explosion of gradients during model training [19,20].

LSTM is a type of Recurrent Neural Network introduced by Hochreiter and Schmidhuber in 1997 [21]. It consists of three types of gates, namely forgetting gates, input gates, and output gates, along with cell states that determine whether to block or pass data and how to process it. LSTM has the ability to capture non-linear and non-stationary time-series information and is particularly well-suited to processing long time-series data with large datasets. This is due to its ability to extract essential information from historical data, selectively remembering important information and forgetting irrelevant information. As a result, it is an effective tool for predicting events with long intervals and lags in time series [22]. In this study, a single LSTM layer is used to extract features from time-series temperature data.

2.3.2. Convolution Neural Network and Transpose Convolution Neural Network

CNN is a type of feedforward neural network with artificial neurons that can respond to part of the surrounding units' coverage. Due to their proficiency in extracting superior features from images by executing convolution, pooling, and full connectivity operations, CNN is extensively applied in image processing. This is attributed to their structural characteristics of local connectivity, weighting, and downsampling [23,24]. Recently, a novel neural network model termed TCNN has been introduced as a variant of CNN typically employed for upsampling to increase the input's height and width and enhance the image resolution [25]. In this study, a 1-layer TCNN is utilized to enlarge the predicted array of fire situation distribution and a 1-layer CNN is used to extract array spatial features, thereby improving fire prediction accuracy.

The AI model employed in this study combines LSTM and CNN algorithms to process sequential temperature data and generate heat maps of temperature, CO, and visibility. The LSTM algorithm captures long-term dependencies in temperature data, while the CNN algorithm extracts spatial features from the heat maps. The amalgamation of these two algorithms enables the model to effectively predict critical fire dynamics and provide essential information for intelligent firefighting decision making.

3. Case Study

3.1. Development of Simulation Models

This section details a fire simulation study conducted in a computer room of a university building information modelling (BIM) laboratory. The simulation model, depicted in Figure 2a, was developed using PyroSim with FDS version 6.7.9, while Figure 2b shows an actual image of the equipment room. Smoke and heat transport of a fire is simulated using a one-step, mixing-controlled combustion model. For easier analysis and comparison, some aspects of the physical structure of the model were simplified. The total volume of the simulated space was 1280 m^3, with a single computational grid size of 0.4 m $\times$ 0.4 m $\times$ 0.4 m. The wall material is set as concrete. The door has a thickness of 0.2 m, and is kept in the 'open' state, while the window is in the natural ventilation state to allow the transfer of air, heat, and smoke. The ambient temperature was set at 20 °C, and there were no mechanical smoke extraction systems or sprinkler systems. Eighty temperature sensors were evenly distributed throughout the room's ceiling at 2 m intervals to monitor temperature distribution. Considering that there are many types of combustible materials in the laboratory, the fire source in the model is set as a 1 m $\times$ 1 m polyurethane burner with a constant heat release rate, and the specific parameter values are kept as the values recommended by FDS. The data acquisition frequency is 1 Hz, i.e., one acquisition per second. The total burning time of each simulation is 300 s. At a horizontal height of 1.6 m, corresponding to the characteristic height of the human eye, the slices of temperature distribution, CO concentration distribution, and smoke visibility distribution were recorded. The size of the array of slices was 21 $\times$ 101.

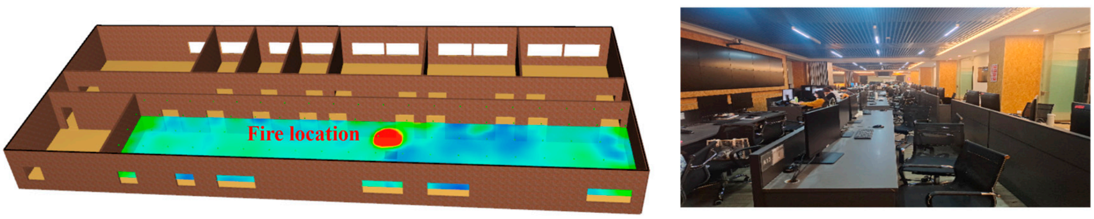

(a) (b)

Figure 2. The laboratory figures. (**a**) Fire simulation model and (**b**) actual picture of the laboratory.

The database of simulated cases considered two main variables: the location of the fire source and the fire severity levels. The purpose is to analyze and compare the fire development characteristics and critical fire development distribution at different fire source locations.

(1) Fire location: A spatial rectangular coordinate system was established, with the room's lower left corner as the origin, for studying fire behavior in the computer room. As shown in Figure 3, twenty fire locations were placed separately in the room at a uniform distance of 4 m.

(2) Fire severity levels: The Heat Release Rate (HRR) is a critical parameter that characterizes the severity levels of a fire. The maximum fire heat release rates corresponding to the different building types are listed in Table 1. Considering the worst case, the maximum heat release rate at steady state in the event of a fire in the laboratory is 10 MW. In order to cover all possible HRR values as much as possible, 12 sets of HRR values uniformly distributed within 10 MW were selected for the study to construct the model dataset. Specifically, HRR values of 0.5, 1, 2, 3.3, 4, 5, 6, 6.7, 7, 8, 9, and 10 MW were set for each of the 20 fire points, resulting in a training dataset consisting of 240 (=20 × 12) scenarios. This approach ensures that the training dataset covers a wide range of fire severity levels and facilitates accurate prediction of fires in the target environment.

Table 1. Maximum heat release rate of different building types.

Building Types	Install Sprinklers	Maximum Heat Release Rate (MW)
Offices, classrooms, guest rooms, walkways	Yes	6.0
	No	1.5
Stores, exhibition halls	Yes	10.0
	No	3.0
Other public places	Yes	8.0
	No	2.5

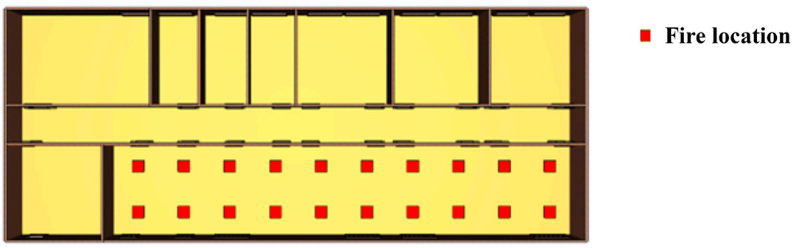

Figure 3. Distribution map of all fire locations in the training set.

Moreover, 60 randomly generated test scenarios were constructed by randomly generating 60 fire location coordinates and 60 heat release rate values within the room coordinate system and a range of heat release rates from 0 to 10 MW. These test scenarios were used to evaluate the fire prediction model.

The training and test databases consist of a total of 300 cases, with each case simulating 300 s of combustion at 1 s intervals. The output includes temporal temperature data tables for 80 temperature sensors and three slice profiles sets representing temperature, CO, and visibility distributions per second. Each slice of data is distributed with 21 × 101 grids of temperature values, CO concentration values, or visibility values. An example of a single scene from the output is shown in Figure 4.

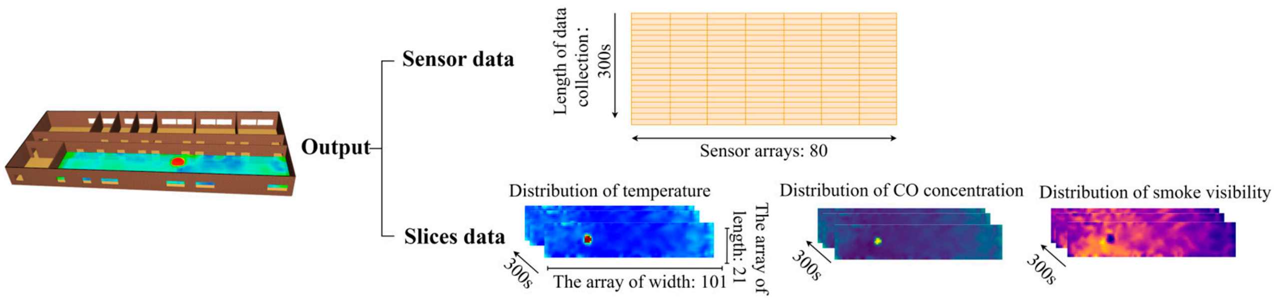

Figure 4. Output data of a single simulated fire scenario.

3.2. Data Preparation for Deep Learning Models

To meet the requirements of the model construction, sliding window processing was used to intercept sequence segments from the time-series data in the sensor data tables. The window size was set to 30, and the sliding step was set to 1, resulting in a time length of 30 s for each sample, with samples taken at 1 s intervals. Thus, the first three samples consisted of data from 1 to 30 s, 2 to 31 s, and 3 to 32 s, respectively, resulting in 212 such data samples per data table as the input. In total, this method generated 50,880 training samples (240 training scenarios × 212 data samples). To ensure independence of the test dataset, it was processed separately following the same approach as the training dataset, resulting in a total of 12,720 test samples (60 test scenarios × 212 data samples). The training dataset was then randomly divided into 38,160 data samples for model training, with the remaining 12,720 samples used for model validation. The test dataset was used to evaluate the accuracy of the deep learning agent model in predicting the fire field. Overall, the proportions of the training, validation, and test datasets were 60%, 20%, and 20% of the total dataset, respectively, as shown in Figure 5a.

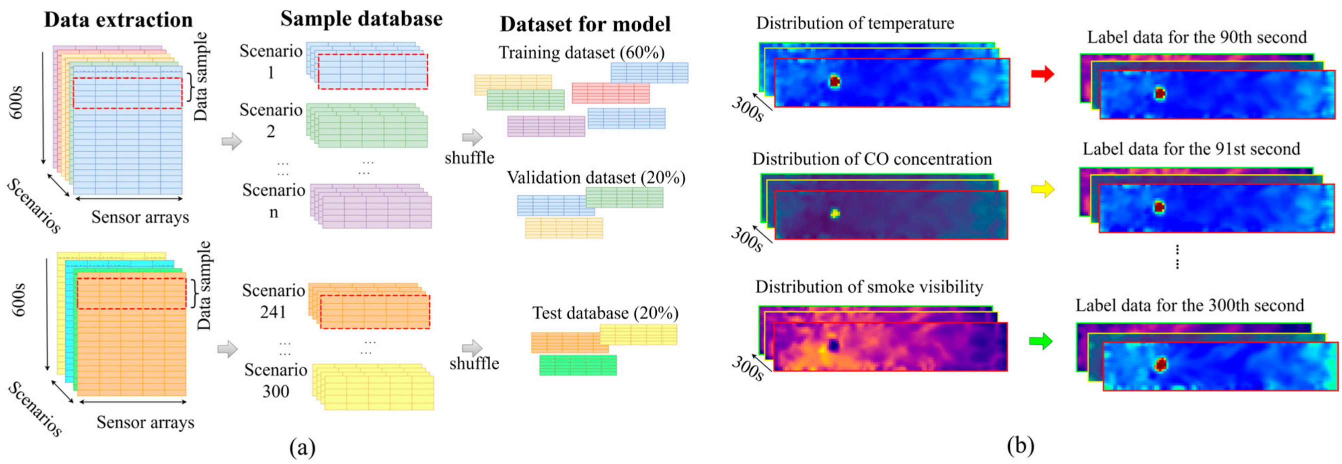

Figure 5. Generation of the training and test database: (**a**) sensor data, (**b**) heat map data.

Three critical fire characteristics were extracted and stored in the form of arrays using the third-party Python package fdsreader. Three characteristics sets of 300 s slice arrays for each scenario were combined every second to generate the label data for the deep learning agent model. For example, the temperature distribution array (shape 21 × 101), the CO concentration distribution array (shape 21 × 101), and the smoke visibility distribution array (shape 21 × 101) at the 90th second were superimposed and combined to form the label data (shape 3 × 21 × 101) for the 1–30 s temperature time-series data, as shown in Figure 5b. Figure 5b shows the heat map obtained from the array.

3.3. Development of Deep Learning Models

The architecture of the AI model network is constructed by employing the PyTorch framework from Python. The fire prediction model takes sensor temperature data with a shape of 30 × 80 (30 s × 80 sensors) as input. The input data are passed through an LSTM layer to extract timing data features, which are then expanded using a fully connected layer. The expanded features are then reshaped and passed through a TCNN layer and a CNN layer. The model outputs a situation distribution array with a shape of 3 × 21 × 101 (i.e., temperature distribution array, CO concentration distribution array, and visibility distribution array), which is mapped into heat maps. The primary structure of the model is depicted in Figure 6.

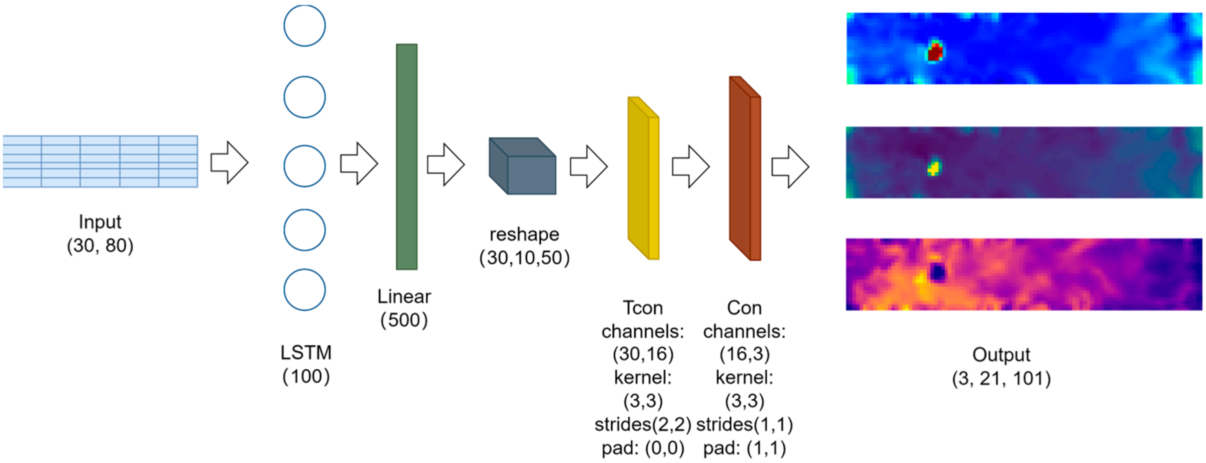

Figure 6. The architecture of the proposed AI model.

The model's performance is significantly influenced by its hyperparameters. This study adopts random weight initialization and the Adam optimization algorithm, with the learning rate set at 0.0001. To avoid overfitting, an EarlyStopping strategy is utilized, whereby the model's training ceases when no reduction is observed in the loss of the validation dataset across 20 continuous epochs.

Random weight initialization is a common practice in deep learning to prevent the model from getting stuck in a local minimum during training by initializing the weights with random values. The Adam optimization algorithm, a popular optimization methodology, is highly compatible for deep neural network training. It amalgamates the benefits of both AdaGrad and RMSProp algorithms, adjusting the learning rate for each weight parameter individually, based on the gradients' first and second moments. The learning rate of 0.0001, a smaller learning rate, helps to prevent the model from taking large steps during gradient descent and potentially overshooting the minimum of the loss function. The EarlyStopping strategy is an approach utilized to avert overfitting of the model to training data. Overfitting occurs when the model becomes too complex and learns the training data extremely well, but is unable to generalize to new data that have not been seen. The early stop strategy stops the model training process if the validation set performance fails to improve after a specific number of epochs. This strategy helps to prevent the model from continuously learning the noise in the training data, thereby improving its ability to generalize to new data.

3.4. Performance Evaluation Metrics

Loss functions and model evaluation metrics are crucial components of machine learning models, serving as the model's accuracy and performance indicators.

The loss function quantifies the error degree between the predicted and actual values in a regression model. Of the available loss functions, the Mean Squared Error (MSE) is a commonly used measure that calculates the squared errors' average between the predicted and actual values, considering the prediction error's variance. Compared to other loss functions, such as Mean Absolute Error (MAE), MSE is more sensitive to deviations between predicted and actual values, thus better guiding the model towards optimal performance. Consequently, MSE is employed as the loss function in this study.

The coefficient of determination, or R^2, is a widely utilized model evaluation metric in regression analysis. R^2 assesses the extent to which a regression model's dependent variable's variability can be explained by the independent variables. Its values range between 0 and 1, with a value closer to 1 denoting better predictive model performance. Compared to other evaluation metrics, such as Root Mean Squared Error and MAE, R^2 offers a more intuitive evaluation result and facilitates a better understanding of the model's predictive power. Moreover, R^2 is highly interpretable and can provide insights into the influence of independent variables on the dependent variable, thereby improving the understanding of the data and the model. Thus, R^2 is selected as the model evaluation index in this paper.

The experimental results show that the R^2 of the predicted temperature distribution, CO distribution, and visibility distribution is about 89.1%, 75.6%, and 84.2%. The overall R^2 is 82.9%. These results indicate that the model is efficient in predicting all three critical fire evolutions.

4. Results and Discussion

In Section 4.1, we investigate the predictive performance of AI models by considering different numbers of sensors and variations in sensor placement. The goal is to determine the most cost-effective sensor number and arrangement that can be applied in real-world scenarios, reducing hardware and software investment while maintaining prediction accuracy. Additionally, we examine the predictive effect of different prediction horizons to ensure reliable predictions. In Sections 4.2–4.4, we select two representative scenarios from 60 test scenarios, called case A and case B. We analyze the predictions of temperature, CO concentration, and visibility fields using AI models under optimal sensor placement. In case A, the ignition source possesses a heat release rate of 2.8 MW, while in case B, it has a heat release rate of 7.4 MW. The location of the fire source also differs between the two cases. These scenarios allow us to visually evaluate the performance of AI models in predicting fire under different conditions.

4.1. Sensor Layout Optimization

Figure 7 shows the model prediction accuracy for different sensor numbers and different locations in the spatial domain. The horizontal axis represents the distance between adjacent sensors on the x-axis, and the vertical axis represents the distance between adjacent sensors on the y-axis. The central value in each box in the figure represents the prediction accuracy, while the red number in the red box in each box denotes the corresponding sensor count. The experiment takes these two values into account to determine the best arrangement of sensor points and the corresponding number.

The coefficient of variation (CV) is calculated by dividing the standard deviation of a dataset by its mean and is used to compare the dispersion of multiple datasets. In general, higher CV values indicate greater dispersion, which makes model prediction more challenging. In this study, the CV values for temperature, CO, and visibility were 0.74, 0.93, and 0.78, respectively. CO distribution was the most difficult to predict, followed by visibility and temperature. These results correspond with the observed trends in Figure 7.

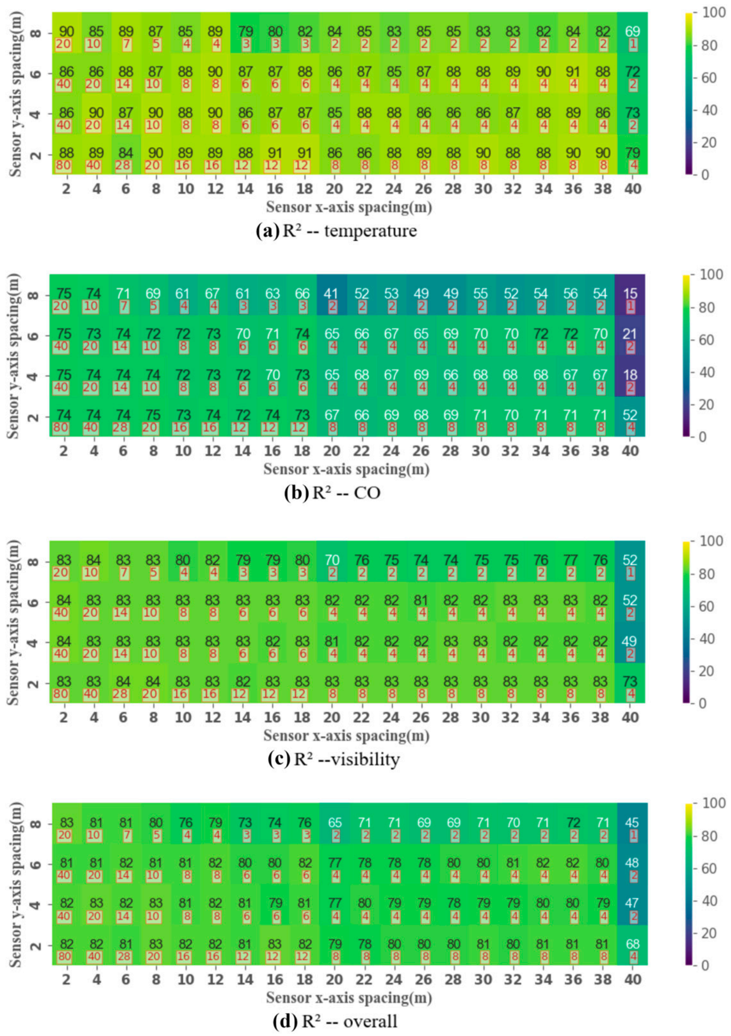

Figure 7. Prediction accuracy of (**a**) temperature distribution, (**b**) CO distribution, (**c**) visibility distribution, and (**d**) overall under different sensor layout.

As can be seen from Figure 7, when more than four sensors are arranged, the overall prediction accuracy can be basically maintained at or above 80%. In addition, when the number of sensors is fixed, the greater the distance between adjacent sensors (especially the *x*-axis), the more accurate the prediction becomes. This may be due to the fact that the temperature data recorded by sensors with greater distances have greater differences and more obvious features, which are more conducive to model prediction. Balancing prediction accuracy and number of sensors, the optimized sensor layout is as follows. Four sensors are placed along the central axis of space, with two columns spaced 36 m apart along the *x*-axis and two rows spaced 6 m apart along the *y*-axis. This optimized layout results in an accuracy of 91% in terms of R^2 for predicting the distribution of temperature distribution, 72% accuracy for predicting CO distribution, and 83% accuracy for predicting visibility distribution. The overall predicted accuracy is approximately 82%. The specific arrangement of measurement points is shown in Figure 8. Figure 9 compares the prediction effect of the AI model with four sensors and eighty sensors. Despite a 20-fold difference in the number of sensors between the two arrangements, both accurately predict the evolution of the fire situation. With the four-sensor arrangement, there may be occasional slight deviations in predicting the fire source point at certain moments. However, the model quickly corrects this error with the input of more time-series data. As expected, the 80-sensor arrangement captures more details of eddies and turbulence due to the larger number of sensors.

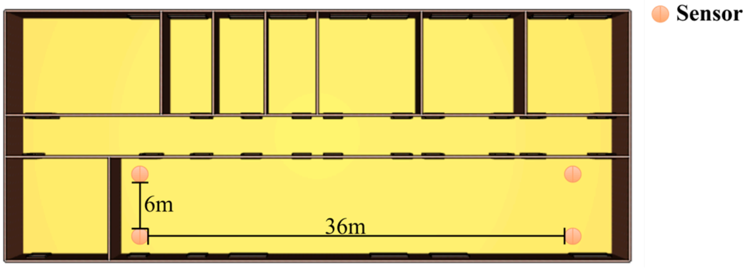

Figure 8. The optimum sensor layout.

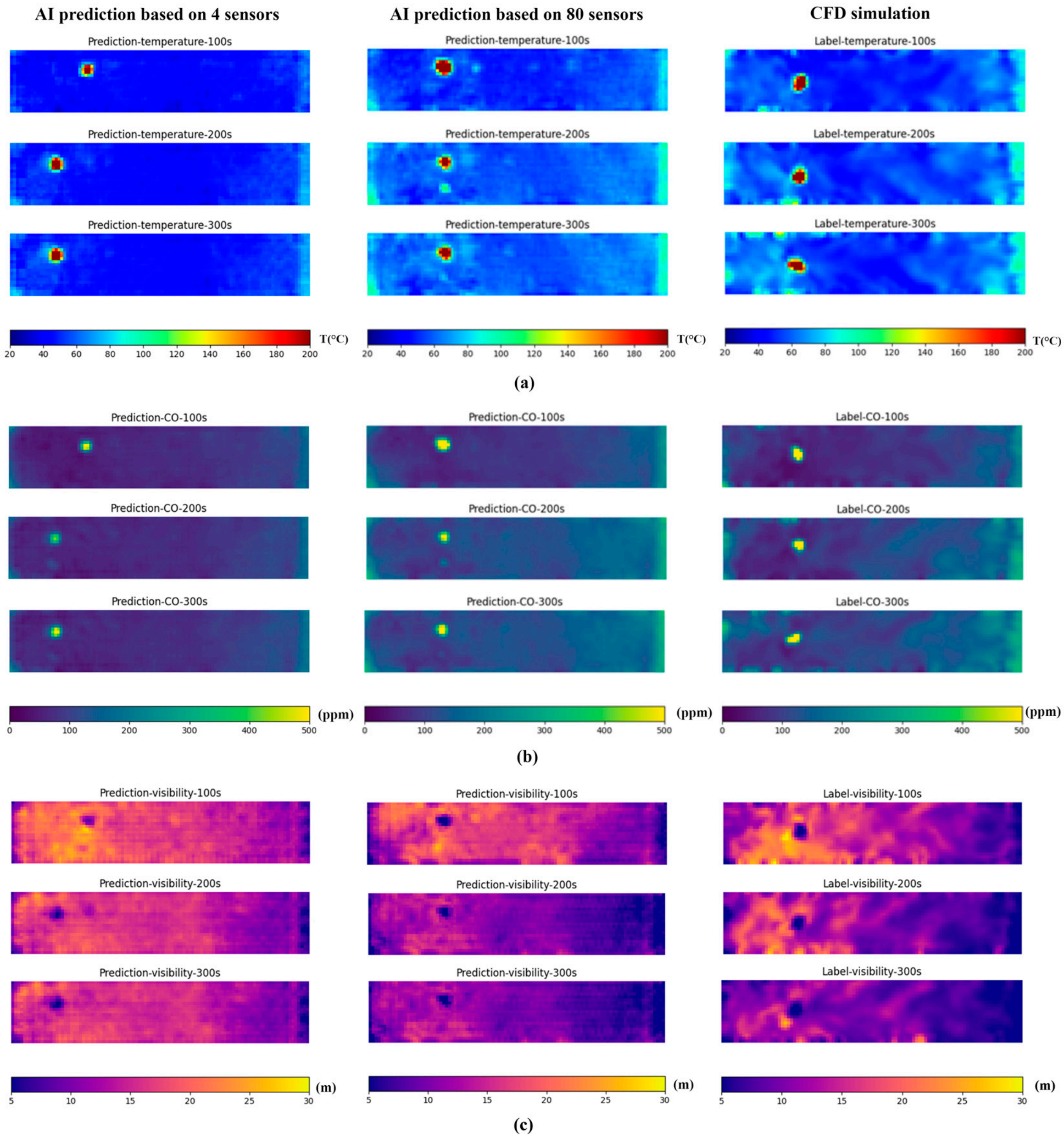

Figure 9. Comparison of prediction effect between 4 sensors and 80 sensors at various time points: 100 s, 200 s, 300 s, including (**a**) temperature distribution, (**b**) CO distribution, and (**c**) visibility distribution.

Based on the optimal arrangement, the prediction effect of different prediction horizons (10 s to 120 s) was further explored. The results show that the influence of prediction horizons on prediction effect is not obvious. This might be due to the relatively stable state of simulated indoor fire situation development over an extended period. Therefore, the influence of prediction horizons on prediction effect is not obvious, as shown in Figure 10.

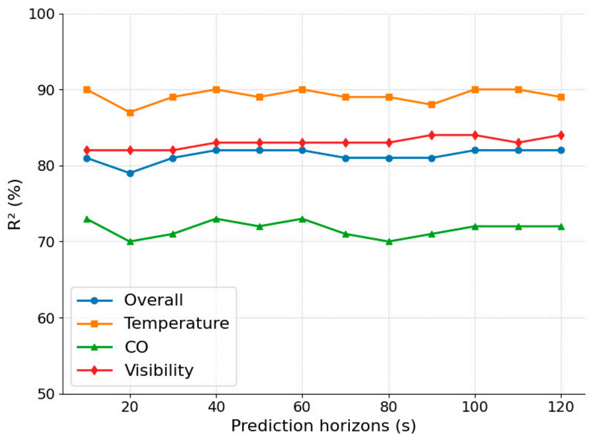

Figure 10. Comparison of prediction effect of different prediction horizons.

Sections 4.2–4.4 compare the prediction effect of temperature distribution, CO distribution, and visibility distribution for 30 s, 60 s, 90 s, and 120 s based on the optimal arrangement.

4.2. Prediction Performance on Spatial Temperature Distributions

This section quantifies the quality of the forecast and the difference between the forecasted and true temperature distributions. Figure 11 shows the model predicted temperature distribution of the 200th and 300th seconds for different prediction horizons and the actual temperature distribution of the simulated data in case A and case B. For visual understanding of the predictions, the temperature array is presented in the form of a heat map. Each colored block corresponds to a numerical value; lower values are shown in blue hues, suggesting cooler temperatures, while higher values are depicted in red hues, indicating warmer temperatures. It is important to note that severe skin burns can occur within one minute in an environment with a temperature of 175 °C [26]. It is assumed that a temperature up to 200 °C is considered safe when firefighters are wearing protective suits. Deep red consistently represents temperatures exceeding 200 °C.

The proposed AI model is effective in predicting the hot areas close to the fire source and the cold areas further away. By counting all the predicted results in a single case, it is concluded that in case A, the average temperature differences after prediction steps of 30 s, 60 s, 90 s, and 120 s are about −12.30 °C, −12.28 °C, −12.30 °C, and −12.68 °C, and the standard deviations are about 31.06 °C, 32.81 °C, 31.52 °C, and 31.98 °C. In case B, the average temperature differences after prediction steps of 30 s, 60 s, 90 s, and 120 s are about −12.82 °C, −13.12 °C, −15.95 °C, and −11.91 °C, and the standard deviations are about 65.35 °C, 64.04 °C, 62.45 °C, and 67.13 °C. As can be seen from the line chart in Figure 11, the accuracy rate is relatively stable with the enlargement of the prediction horizon, showing no increasing or decreasing trend.

However, the model appears to be biased in its ability to predict the precise location of the fire source. As can be seen from the figure, there are deviations in the prediction of the high-temperature region of the temperature field. This is attributable to the fire source locations in the test set being randomly generated, in contrast to the fixed 20 fire source locations used during model training. Models tend to bias towards known data when encountering unknown data, which explains the observed deviation in the model's prediction of the fire source's high-temperature region. Expanding the training set is expected to improve the model's performance in handling such scenarios. At the same time, the position of the high-temperature fire source shown by the forecast results is not fixed, because the plume will sway and tilt under the influence of local airflow [27], so there will be obvious deviations. In practice, the model's prediction of the ignition source is usually off by no more than 3 m, usually within the acceptable range. As stated earlier, AI models struggle to predict complex fire behavior such as convection and turbulence.

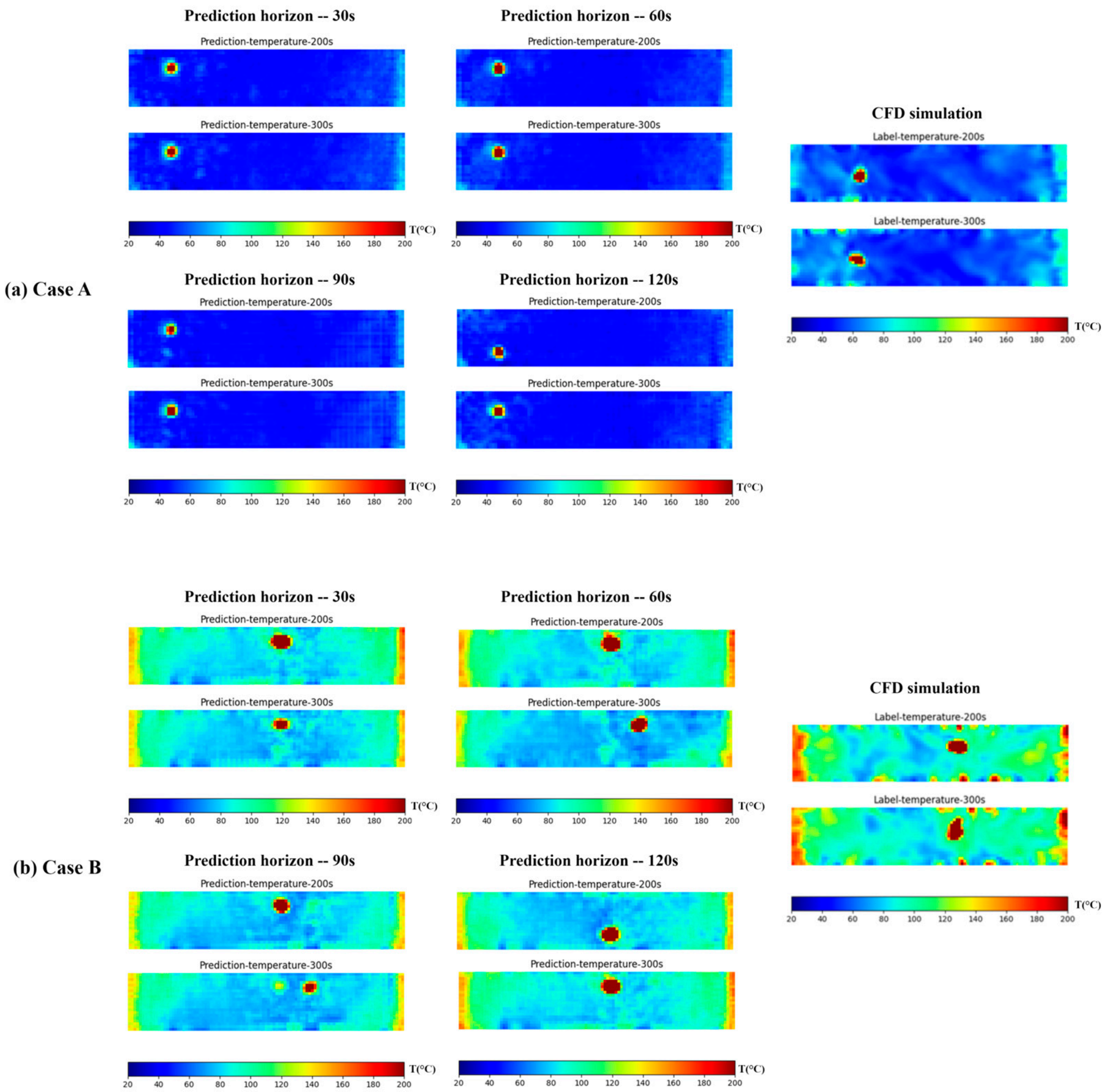

Figure 11. Comparison of predicted and actual temperature distributions at 200 s and 300 s for different prediction horizons and their differences include: (**a**) case A, (**b**) case B.

4.3. Prediction Performance on Spatial CO Distributions

Figure 12 shows the CO concentration distribution predicted by the model at the 200th and 300th seconds, considering different prediction horizons. It also shows the actual distribution of the simulated data, visualizing the discrepancy between the model predictions and the actual data in both scenarios. Arrays in the shape of 21×101 are represented as heat maps, with each color block representing a numerical value. Purple colors represent lower CO concentrations, while yellow indicates higher concentrations. The risk threshold for human life concerning CO is generally set at 500 ppm, with concentrations exceeding 500 ppm consistently shown in yellow.

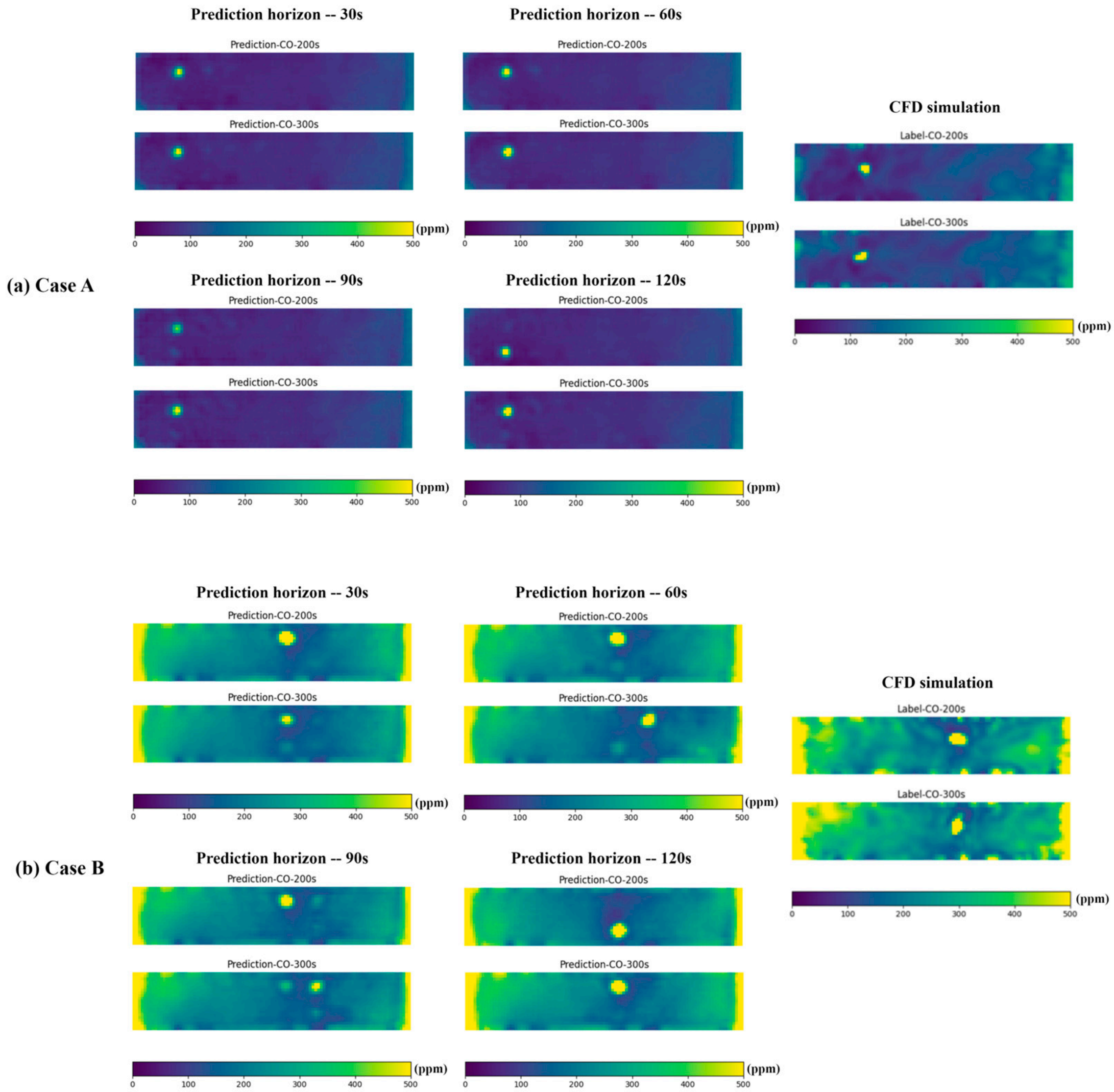

Figure 12. Comparison of predicted and actual CO distributions at 200 s and 300 s for different prediction horizons and their differences include: (**a**) case A, (**b**) case B.

The proposed artificial intelligence model demonstrates effective prediction of CO concentration distribution in fire scenarios. Specifically, in case A, the average CO concentration difference after 30 s, 60 s, 90 s, and 120 s between the predicted and simulated values is approximately −39.54 ppm, −37.32 ppm, −39.15 ppm, and −39.11 ppm, with a standard deviation of about 78.17 ppm, 80.37 ppm, 79.24 ppm, and 81.88 ppm, respectively. In case B, the average CO concentration difference after 30 s, 60 s, 90 s, and 120 s is approximately −47.63 ppm, −44.01 ppm, −54.02 ppm, and −47.37 ppm, with a standard deviation of about 182.80 ppm, 182.16 ppm, 181.83 ppm, and 185.33 ppm, respectively. These findings demonstrate that the model does a relatively good job of forecasting the distribution of CO concentrations and accurately predicting the overall trend. Similarly, the line chart in Figure 12 indicates the relatively stable accuracy rate with the enlargement in the prediction horizon, showing no ascending or descending trend.

However, the model exhibits a bias in predicting high CO concentrations near the fire source. This is due to the randomness of the test set and the instability of the flame. Furthermore, the model's performance in predicting complex convection and turbulent flow behaviors is not optimal. These factors influence the model's ability to predict high-

CO-concentration areas. Further research is needed to enhance the model or to introduce expert knowledge to strengthen the predictive ability for complex fire scenarios.

4.4. Prediction Performance on Spatial Visibility Distributions

Figure 13 illustrates the predictive performance of the model for smoke visibility distribution at the 200th and 300th seconds across various prediction horizons, along with the corresponding differences. The model predictions are compared with the reality of the simulated data for different fire source locations and randomly generated heat release rates. The heat maps comprise 21 × 101 arrays, with each color block representing a numerical value. Deep blue represents lower visibility values, while yellow represents higher visibility values. Visibility is a critical factor for safe evacuation, and the visibility threshold for smaller spaces, such as an office building, should not be less than 5 m. In the heat maps, visibility values below 5 m are shown in deep blue.

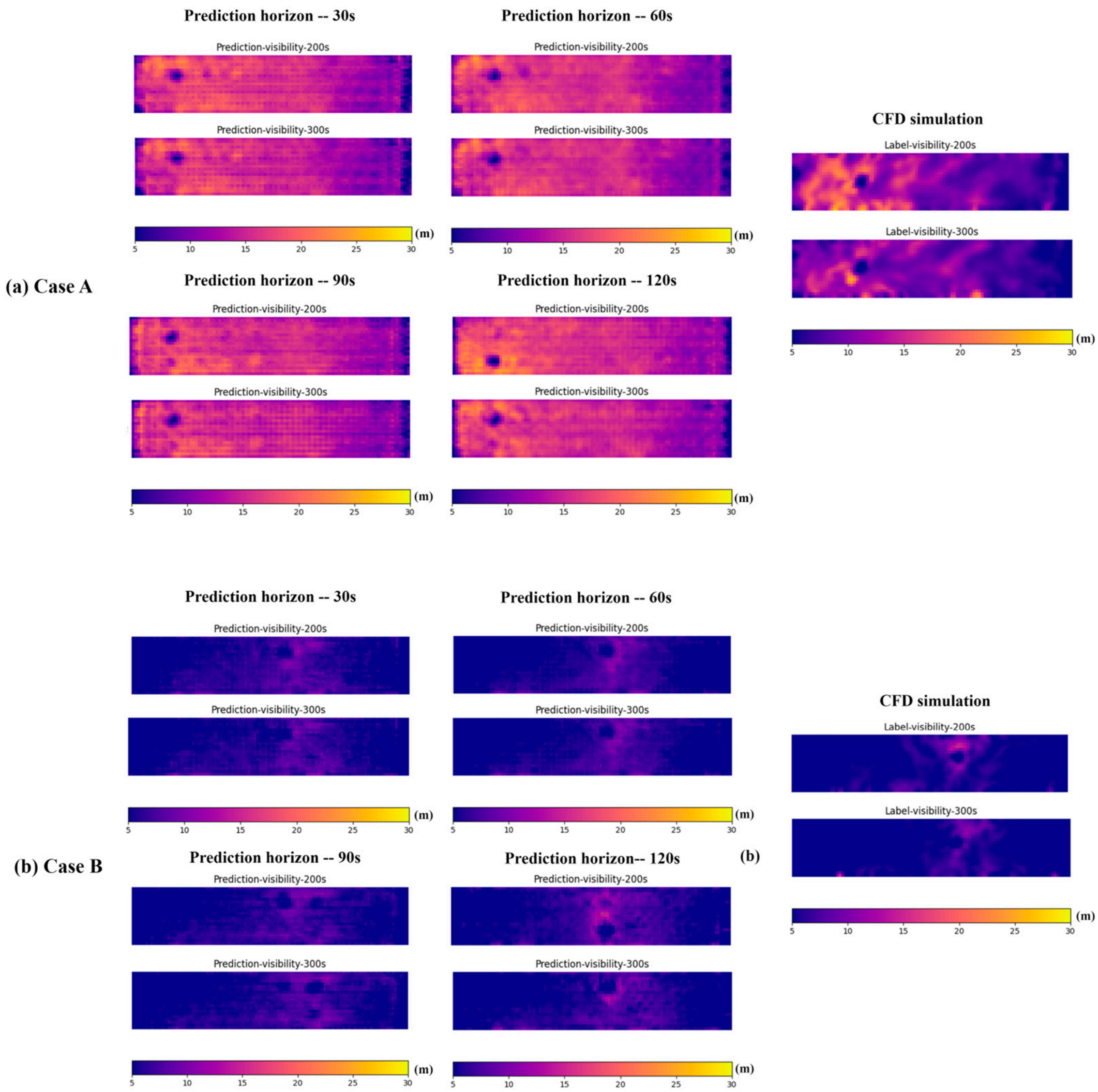

Figure 13. Comparison of predicted and actual visibility distributions at 200 s and 300 s for different prediction horizons and their differences include: (**a**) case A, (**b**) case B.

The experimental results show that the proposed AI model is effective in predicting the distribution of visibility in fire scenarios. Specifically, in case A, the mean difference between the predicted and simulated values of visibility is approximately −0.35 m, 0.69 m, 1.92 m, and −3.07 m, with a standard deviation of approximately 6.91 m, 6.12 m, 5.03 m, and 5.24 m. In case B, the mean difference in visibility is approximately −1.50 m, −0.37 m, −0.46 m, and 0.09 m, with a standard deviation of approximately 4.56 m, 3.68 m, 3.64 m, and 3.48 m. These results suggest that the model is capable of accurately predicting overall trends and performs well in predicting visibility distributions. Similarly, it can be seen from the chart in Figure 13 that the accuracy rate is relatively stable with the expanding of the prediction horizons, without displaying an increasing or decreasing trend.

The model's prediction of visibility is slightly more accurate than its prediction of temperature and CO concentration distributions, and still provides essential information for fire safety analysis. Nevertheless, the model predictions may contain some errors, which are generally within acceptable limits and do not significantly affect the overall prediction. The sophisticated nature of convection and turbulent behavior is difficult for the AI model to learn. In order to improve the predictive ability of the model, it is recommended to improve its training on more cases and to collect more training data to improve the adaptability and generalization of the model. In addition, the predictive performance of the model can be improved by incorporating more refined physical models and advanced algorithms.

5. Conclusions

This study proposes a deep learning model for predicting indoor fires in advance and established an optimization method for the layout of fire sensor systems based on a deep learning agent model. The goal is to predict the distribution of temperature, CO concentration, and smoke visibility in advance using an optimized sensor system layout, providing support for intelligent fire decision making.

To validate the approach, the researchers built a database of 300 indoor fire scenarios based on a lab, which varied in fire location and heat release rate. A fused neural network model incorporating LSTM, TCNN, and CNN was developed to output arrays of temperature, CO concentration, and smoke visibility distribution based on input temperature series data from temperature sensors. By varying the input information of the AI model, the impact of different spatial layouts of sensors and different prediction horizons on the fire situation prediction is investigated.

The major findings are as follows.

- The number and arrangement of sensors significantly influence the prediction accuracy. The optimization results suggest that if four sensors are evenly spaced around the room, with an x-interval of 36 m and a y-interval of 6 m, the overall prediction accuracy will be greater than 80%. The optimized sensor system layout can significantly reduce the number of sensor layouts while maintaining effective prediction, consequently reducing the total cost of equipment investment.
- The prediction horizon has no significant effect on the prediction accuracy. This may be because the indoor fire development simulated in this study is relatively stable, and the prediction effect under different prediction horizons is basically the same.

Despite some biases, the model demonstrates satisfactory accuracy in predicting major fire developments, providing valuable information about the fire scene. However, the model's ability to predict fire turbulence and convection behavior is limited, potentially due to a lack of expert input.

Beyond the particular scenario discussed above, the research methodology outlined in this paper can be applied to various scenarios to achieve an improved sensor layout. In such cases, we would recommend re-evaluating the sensor distribution through protocols proposed in this study. The study underscores the potential of AI models for practical applications to predict the evolution of critical indoor fires, significantly contributing to our ability to monitor and predict such fires. Furthermore, the application of AI models in firefighting decisions promises to reduce the threat of fire to human life and property substantially, such as in combination with path planning to plan escape and rescue routes in advance.

6. Limitations and Future Research

The limitations of the study and potential directions for future research are as follows.

1. Scope of fire scenarios: The study focuses on basic fire scenarios, but fire scenarios in practice are more complex, as they include factors such as hidden spaces and attics. The model's ability to generalize to more complex scenarios is limited. Future research should aim to train AI models on a wider range of fire scenarios to enhance their applicability and generalization.
2. Lack of experimental data: The study relied on CFD simulations instead of real experimental data for model validation. While CFD simulations are valuable for understanding various aspects of indoor fire scenarios, they may not fully capture the complexity of certain factors, such as CO generation during combustion. CO generation is known to be sensitive to factors like fuel type and combustion conditions, which can vary widely in real-world fire incidents. Incorporating a broader range of experimental data, particularly data related to CO generation, would improve the accuracy and generalizability of the deep learning model. Future research should strive to obtain measured data (e.g., fire field slice data) from real fire incidents for validation purposes.
3. Collaborative data collection: Collaborating with researchers, firefighters, and stakeholders is essential for gathering diverse and comprehensive real-world fire incident data. By involving domain experts and incorporating their input, future models can better address the challenges and complexities of firefighting, leading to more accurate predictions.
4. Model interpretability: Deep learning models are often seen as black boxes, hindering the interpretation of underlying decision-making processes. In critical domains like firefighting, understanding the rationale behind predictions is crucial. Future research should explore techniques to enhance interpretability and transparency, enabling stakeholders to better comprehend and trust the model's outputs.

In conclusion, the study makes a valuable contribution to the field of fire prediction using deep learning techniques. However, it is important to acknowledge and address the limitations associated with scenario representation, data availability, model generalization, and interpretability. These limitations highlight areas for further research and collaborative efforts to advance the accuracy, applicability, and transparency of fire modeling and prediction. By addressing these limitations, we can improve the effectiveness of deep learning models in predicting and managing fire incidents, ultimately enhancing safety and decision making in firefighting scenarios.

Author Contributions: Conceptualization, C.F.; Data curation, L.Z.; Funding acquisition, C.F., H.Z. and Y.Z.; Investigation, L.Z. and Y.Z.; Methodology, C.F.; Project administration, L.M., H.Z. and Y.Z.; Resources, L.M.; Software, L.Z. and C.F.; Supervision, H.Z.; Visualization, L.M.; Writing—original draft, L.Z. and C.F.; Writing—review and editing, H.Z. All authors have read and agreed to the published version of the manuscript.

Funding: This study was supported by the National Key R&D Program of China (Grant No. 2020YFB2103503), the Philosophical and Social Science Program of Guangdong Province, China (GD22XGL20), and the Shenzhen Science and Technology Program (No. 20220531101800001 and 20220810160221001).

Institutional Review Board Statement: Not applicable.

Informed Consent Statement: Not applicable.

Data Availability Statement: Datasets used during the current study are available from the corresponding author on reasonable request.

Conflicts of Interest: The authors declare that they have no known competing financial interest or personal relationships that could have appeared to influence the work reported in this paper.

References

1. Klepeis, N.E.; Nelson, W.C.; Ott, W.R.; Robinson, J.P.; Tsang, A.M.; Switzer, P.; Behar, J.V.; Hern, S.C.; Engelmann, W.H. The National Human Activity Pattern Survey (NHAPS): A resource for assessing exposure to environmental pollutants. *J. Expo. Sci. Environ. Epidemiol.* **2001**, *11*, 231–252. [CrossRef] [PubMed]
2. Zhang, Z.; Lu, T.; Yang, D.; Lu, S.; Cai, R.; Tan, W. A Dual-Function Sensor for Highly Sensitive Detection of Flame and Humidity. *Small* **2022**, *18*, e2203334. [CrossRef]
3. Chew, M.Y.L.; Yan, K. Enhancing Interpretability of Data-Driven Fault Detection and Diagnosis Methodology with Maintainability Rules in Smart Building Management. *J. Sens.* **2022**, *2022*, 5975816. [CrossRef]
4. Elsisi, M.; Tran, M.-Q.; Mahmoud, K.; Lehtonen, M.; Darwish, M.M.F. Deep Learning-Based Industry 4.0 and Internet of Things Towards Effective Energy Management for Smart Buildings. *Sensors* **2021**, *21*, 1038. [CrossRef] [PubMed]
5. Rejeb, A.; Rejeb, K.; Simske, S.; Treiblmaier, H.; Zailani, S. The big picture on the internet of things and the smart city: A review of what we know and what we need to know. *Internet Things* **2022**, *19*, 100565. [CrossRef]
6. Li, E.; Zhang, W. Smoke Image Segmentation Algorithm Suitable for Low-Light Scenes. *Fire* **2023**, *6*, 217. [CrossRef]
7. James, G.L.; Ansaf, R.B.; Al Samahi, S.S.; Parker, R.D.; Cutler, J.M.; Gachette, R.V.; Ansaf, B.I. An Efficient Wildfire Detection System for AI-Embedded Applications Using Satellite Imagery. *Fire* **2023**, *6*, 169. [CrossRef]
8. Ryu, J.; Kwak, D. A Study on a Complex Flame and Smoke Detection Method Using Computer Vision Detection and Convolutional Neural Network. *Fire* **2022**, *5*, 108. [CrossRef]
9. Starr, J.W.; Lattimer, B.Y. Evaluation of Navigation Sensors in Fire Smoke Environments. *Fire Technol.* **2014**, *50*, 1459–1481. [CrossRef]
10. Wu, H.; Wu, D.; Zhao, J. An intelligent fire detection approach through cameras based on computer vision methods. *Process. Saf. Environ. Prot.* **2019**, *127*, 245–256. [CrossRef]
11. Su, L.-C.; Wu, X.; Zhang, X.; Huang, X. Smart performance-based design for building fire safety: Prediction of smoke motion via AI. *J. Build. Eng.* **2021**, *43*, 102529. [CrossRef]
12. Wu, X.; Zhang, X.; Huang, X.; Xiao, F.; Usmani, A. A real-time forecast of tunnel fire based on numerical database and artificial intelligence. *Build. Simul.* **2022**, *15*, 511–524. [CrossRef]
13. Li, J.; Liu, W.; Li, Y.; Chow, W.; Chow, C.; Cheng, C. Scale modelling experiments on the effect of longitudinal ventilation on fire spread and fire properties in tunnel. *Tunn. Undergr. Space Technol.* **2022**, *130*, 104725. [CrossRef]
14. Manea, F.; Ghicioi, E.; Suvar, M.C.; Prodan, M.; Vlasin, N.I.; Suvar, N.S.; Vlase, T. FDS Results for Selecting the Right Scenario in the Case of a Building Fire: A Case Study. *Fire* **2022**, *5*, 198. [CrossRef]
15. Ryder, N.L.; Sutula, J.A.; Schemel, C.F.; Hamer, A.J.; Van Brunt, V. Consequence modeling using the fire dynamics simulator. *J. Hazard. Mater.* **2004**, *115*, 149–154. [CrossRef]
16. Chi, J.-H. Reconstruction of an Inn Fire Scene Using the Fire Dynamics Simulator (FDS) Program. *J. Forensic Sci.* **2013**, *58*, S227–S234. [CrossRef]
17. Janardhan, R.K.; Hostikka, S. Predictive Computational Fluid Dynamics Simulation of Fire Spread on Wood Cribs. *Fire Technol.* **2019**, *55*, 2245–2268. [CrossRef]
18. Shen, T.-S.; Huang, Y.-H.; Chien, S.-W. Using fire dynamic simulation (FDS) to reconstruct an arson fire scene. *Build. Environ.* **2008**, *43*, 1036–1045. [CrossRef]
19. Sherstinsky, A. Fundamentals of Recurrent Neural Network (RNN) and Long Short-Term Memory (LSTM) Network. *Phys. D Nonlinear Phenom.* **2020**, *404*, 132306. [CrossRef]
20. Sayah, M.; Guebli, D.; Al Masry, Z.; Zerhouni, N. Robustness testing framework for RUL prediction Deep LSTM networks. *ISA Trans.* **2021**, *113*, 28–38. [CrossRef]
21. Zhou, H.; Zhang, Y.; Yang, L.; Liu, Q.; Yan, K.; Du, Y. Short-Term Photovoltaic Power Forecasting Based on Long Short Term Memory Neural Network and Attention Mechanism. *IEEE Access* **2019**, *7*, 78063–78074. [CrossRef]
22. Bedi, J.; Toshniwal, D. Deep learning framework to forecast electricity demand. *Appl. Energy* **2019**, *238*, 1312–1326. [CrossRef]
23. Alzubaidi, L.; Zhang, J.; Humaidi, A.J.; Al-Dujaili, A.; Duan, Y.; Al-Shamma, O.; Santamaría, J.; Fadhel, M.A.; Al-Amidie, M.; Farhan, L. Review of deep learning: Concepts, CNN architectures, challenges, applications, future directions. *J. Big Data* **2021**, *8*, 53. [CrossRef] [PubMed]
24. Gao, H.; Yuan, H.; Wang, Z.; Ji, S. Pixel Transposed Convolutional Networks. *IEEE Trans. Pattern Anal. Mach. Intell.* **2020**, *42*, 1218–1227. [CrossRef] [PubMed]
25. Hodges, J.L.; Lattimer, B.Y.; Luxbacher, K.D. Compartment fire predictions using transpose convolutional neural networks. *Fire Saf. J.* **2019**, *108*, 102854. [CrossRef]
26. How High a Temperature Can Human Skin Tolerate. Available online: https://www.gov.cn/yjgl/2005-07/31/content_18872.htm (accessed on 31 July 2005).
27. Zhang, T.; Wang, Z.; Zeng, Y.; Wu, X.; Huang, X.; Xiao, F. Building Artificial-Intelligence Digital Fire (AID-Fire) system: A real-scale demonstration. *J. Build. Eng.* **2022**, *62*, 105363. [CrossRef]